Mater. Res. Soc. Symp. Proc. Vol. 1369 © 2012 Materials Research Society
DOI: 10.1557/opl.2012.509

Development and Application of Chen-Mobius Lattice Inversion Potential for Pd-Au Alloy

Xianbao Duan,[1] Zhengzheng Chen,[1] Neeti Kapur,[2] Xianghong Hao,[2] Kyeongjae Cho,[3] and Bin Shan[1,2*]
[1]School of Materials Science and Engineering, Huazhong University of Science and Technology, Wuhan 430074, Hubei, People's Republic of China
[2]Nanostellar Inc, 3696 Haven Ave, Redwood City, CA 94063, U.S.A.
[3]Department of Materials Science and Engineering, The University of Texas at Dallas, Richardson, TX 75080, U.S.A.
*Corresponding author: bshan@mail.hust.edu.cn

ABSTRACT

Bimetallic Pd-Au nanoparticles have received much attention due to their potential applications in catalysis. We have developed a Pd-Au alloy potential based on Chen-Mobius lattice inversion method and applied it to the investigation of the melting of Pd-Au binary nanoparticles via molecular dynamics simulations. Our simulation results show the particle size dependence of the melting point and an enrichment of Au atoms to the surface near melting temperature.

INTRODUCTION

Bimetallic nanoparticles (NPs) have found wide applications in many practical areas such as vehicle exhaust gas after-treatments[1]. As one kind of prototype, Pd-Au NPs have received much attention because they are promising top-performance catalysis for NO_x and/or CO_x oxidation[2]. Furthermore, Pd-Au NPs have desirable resistance against bulk oxide or sulfide formation in realistic engine operating conditions. Experimental observations have demonstrated that surface morphology and species constitutes a play key role in determining NPs' catalytic performance. Though extensive studies based on density functional theory (DFT) calculations have been reported, the microscopic catalytic mechanism still remains controversial. One difficulty against the full understanding is that the computational cost of DFT calculations on NPs, which contain $10^2 \sim 10^5$ atoms, are prohibitively expensive. Unfortunately, models with too limited sizes cannot take into account the effects of defects, segregation, etc. which are essential to the understanding of reaction mechanism. Therefore, methods based on empirical potentials could shed light on studies regarding to NPs with more realistic structures and sizes. Though assorted empirical potentials have been developed and reported [3, 4], the transferability and accuracy of these potentials are still limited and the morphology and thermodynamic stability of Pd-Au NPs are not well understood. Chen-Mobius lattice inversion formula, developed by Chen [5], has been employed on different metal and/or alloy systems and has several advantages over previous empirical potentials. This analytic method based on number theory requires no presetting format of atomic interactions compared with other empirical potentials, such as Morse potential or Lennard-Jones potential, and thus is more general for systems with diverse structures. In this study, we report the development of a binary pair potential based on Chen-Mobius lattice inversion method, that exactly reproduces the DFT cohesive energy curves of Pd, Au, and Pd-Au $L1_0$ alloy structure. We had also applied molecular dynamics (MD) simulations to investigate the dependence of the melting point of Pd-Au NPs on particle sizes and analyzed the particle morphology as a function of temperature.

THEORY

1. Chen-Mobius Lattice Inversion Potential

Chen-Mobius inversion formula was first derived by NanXian Chen [5] in 1990 based on the number theory and has been extended to multidimensional inverse lattice problems in condensed matter physics successfully [6]. The lattice inversion potentials are constructed such that the interatomic potentials can be derived from the cohesive energy curve accurately with only moderate computational cost. In the past years, Chen-Mobius lattice inverse formulas for many different structures have been derived [6-9].

In this work, we used the cohesive energy curves from DFT calculations as the starting point for Chen-Mobius lattice inversion. Vienna Ab Initio Simulation Package (VASP) [10] was used to obtain the cohesive energies of pure Pd, Au and Pd-Au $L1_0$ binary alloy, respectively. The projected augmented wave approach was used to represent the electron-ion interaction and Perdew-Burke-Erzenhof functional [10] as exchange-correlation functional. A $16\times16\times16$ K-point mesh was set to sample the first Brillouin zone according to Monkhost-Pack scheme. The optimized lattice constants for Pd and Au were 3.94 and 4.19 Å, which are in good agreement with experimental values of 3.89 and 4.08 Å, respectively.

Theoretically speaking, any cohesive energy $E(x)$ can be expressed as a sum of many-body interactions. If only two-body interactions $\Phi(x)$ are considered:

$$E(x)=\frac{1}{2}\sum_{R\neq0}\Phi(R), \tag{1}$$

where x is the nearest neighbor distance, R represents all the possible lattice vectors. For convenience, the potential function $\Phi(R)$ can be expressed as $r_0(n)\Phi\left(b_0(n)\,x\right)$. So Eq. (1) can be written as:

$$E(x)=\frac{1}{2}\sum_{n=1}^{\infty}r_0(n)\Phi\left(b_0(n)\,x\right), \tag{2}$$

where $r_0(n)$ is the number of the n^{th} set of lattice points; $b_0(n)$ is a series which represents the distance between the original atom as the reference and the n^{th} set of lattice points, where n approaches infinity.

In order to perform the Chen-Mobius inversion, we extend the series $\{b_0(n)\}$ to a multiplicative closeness $\{b(n)\}$. Thus Eq. (2) can be transformed to the following:

$$E(x)=\frac{1}{2}\sum_{n=1}^{\infty}r(n)\Phi\left(b(n)\,x\right), \tag{3}$$

where

$$r(n)=\begin{cases}r_0\left(b_0^{-1}\left[b(n)\right]\right) & b(n)\in b_0(n)\\ 0 & b(n)\notin b_0(n)\end{cases}. \tag{4}$$

According to the Chen-Mobius inversion, the solution to Eq. (3) is given by

$$\Phi(x)=2\sum_{n=1}^{\infty}I(n)E\left(b(n)\,x\right), \tag{5}$$

where the inversion coefficient $I(n)$ is given by

$$\sum_{b(n)|b(k)} I(n) r\left(b^{-1}\left[\frac{b(k)}{b(n)} \right] \right) = \delta_{k1}\,, \tag{6}$$

where δ_{k1} is Kronecker delta function.

2. Molecular Dynamics Simulation for Pd-Au NPs Melting

We used LAMMPS [11, 12] to perform MD simulations. Five Pd-Au NPs with the number of atoms equal to 55, 147, 309, 561, 923, respectively, were researched. Non-periodic boundary condition was employed to mimic the finite size and free facets of NPs. We used canonical ensemble, and performed MD simulations at different temperatures changing from 100 to 2,000 K with interval as 100 K. The time step was set to 2 fs. For each calculation, we spent 40 ps to get thermodynamic equilibrium for each NP, and then statistical data was gathered over 160ps.

There is a well defined melting point to separate solid and liquid phases in bulk materials, which depends on temperature and pressure. In the case of NPs, however, the melting point depends on the particle size. There are various properties to characterize the melting point, such as *Lindemann index*, static structure factors, radial distribution functions, etc. In the present work, we employed *Lindemann index* [13-15], δ which is defined as

$$\delta = \frac{2}{N(N-1)} \sum_{i<j} \frac{\sqrt{\left\langle r_{ij}^2 \right\rangle_t - \left\langle r_{ij} \right\rangle_t^2}}{\left\langle r_{ij} \right\rangle_t}\,, \tag{7}$$

where r_{ij} is the distance between atom *i* and atom *j*, N is number of atoms, $\langle\ \rangle_t$ indicates a time average. The melting temperature is characterized by a sudden jump in *Lindemann index* as a function of temperature.

RESULTS AND DISCUSSION

1. Inversion potentials of Pd-Pd and Au-Au

For FCC structure, $b(n)$ and $I(n)$ have been reported in many previous literatures [6] and are tabulated in Table I. According to the Chen-Mobius lattice inverse formula, $\Phi(x)$ can be expressed as the following:

$$\Phi(x) = 2\left[\frac{1}{12}E(x) - \frac{1}{24}E(\sqrt{2}x) - \frac{1}{6}E(\sqrt{3}x) - \frac{1}{16}E(2x) - \frac{1}{6}E(\sqrt{2}x) + \ldots \right]. \tag{8}$$

In order to evaluating the cohesive energies of Pd and Au within the nearest neighbor distance from 2.8 to 6.5 Å, we employed a cubic *spline* interpolation function. Outside this region, two approximate functions were adopted, shown as the following:

$$E(a) = \begin{cases} C/a^n & 0 < a < a_{\min} \\ \text{interpolation} & a_{\min} \le a \le a_{\max} \\ Ae^{-Ba} & a > a_{\max} \end{cases} \tag{9}$$

where the coefficients *A*, *B*, *C*, and *n* were calculated to ensure C1 continuity at a_{min} and a_{max}. After the preparation of cohesive energies and relative coefficient series, the interatomic potentials of Pd-Pd and Au-Au can be obtained by solving Chen-Mobius inverse formula. The formula consists of infinite terms and only the leading 10 terms were calculated here, which was

proved to achieve reasonable accuracy. The developed potential curves are shown in Figure 1(a). We can see that Pd-Pd bonds are generally stronger than Au-Au bonds across the whole range.

Table I. Related coefficient series of Chen-Mobius inverse formula for FCC structure

n	1	2	3	4	5	6	7	8	9	10
$[b(n)]^2$	1	2	3	4	5	6	7	8	9	10
$r(n)$	12	6	24	12	24	8	48	6	36	24
$I(n)$	1/12	-1/24	-1/6	-1/16	-1/6	1/9	-1/3	1/32	1/12	0

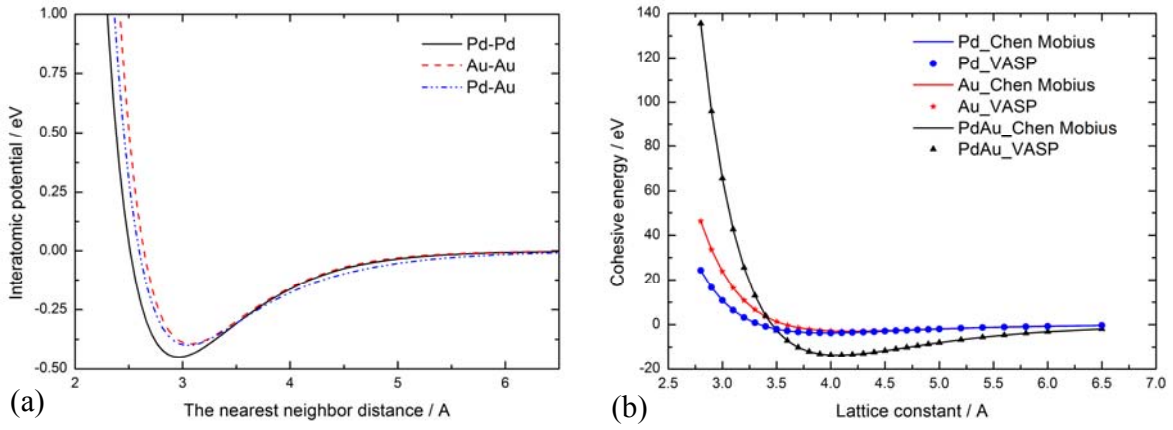

Figure 1. (Color online) (a) Interatomic potential of Pd-Pd, Au-Au and Pd-Au developed by Chen-Mobius lattice inversion method (b) Comparison of cohesive energy of Pd, Au and Pd-Au binary alloy from DFT calculations and from Chen-Mobius inversion potentials

2. Inversion potential of Pd-Au

In order to obtain the interatomic potential for Pd-Au, a reference structure including Pd and Au should be constructed. Here Pd-Au alloy with $L1_0$ super structure was chosen for simplicity. With the presence of 2 Pd atoms and 2 Au atoms in a unit cell for Pd-Au, the total system energy can be decomposed into three individual interaction, including Pd-Pd, Au-Au, and Pd-Au bonds. From above we derived the Pd-Au component:

$$E_{Pd-Au} = E_{total} - E_{Pd-Pd} - E_{Au-Au} \tag{10}$$

where E_{total} is total energy of the unit cell; E_{Pd-Pd} and E_{Au-Au} are the cohesive energies of Pd-Pd and Au-Au with $L1_0$ super structure, respectively, which can be easily calculated by adding up the interatomic potentials obtained above based on Eq. (2).

By appropriately counting the hetero-pairs of Pd-Au bonds in $L1_0$ super structure, related coefficient series in the Chen-Mobius inverse formula are tabulated in Table II. When calculating $b_0(n)$ or $r_0(n)$ for Pd-Au alloy, only the bonds between hetero-pairs are counted. For example, if an arbitrary Pd (or Au) atom was selected as the reference atom, then only Au (or Pd) atoms were considered when counting the n^{th} nearest neighbor.

The Chen-Mobius inverse formula for $L1_0$ super structure can be given as the following:

$$\Phi(x) = 2\left[\frac{1}{8}E(x) - \frac{1}{4}E(\sqrt{3}x) - \frac{1}{4}E(\sqrt{5}x) - \frac{1}{2}E(\sqrt{7}x) - \frac{1}{8}E(3x) + \ldots\right] \tag{11}$$

The developed pair potential for Pd-Au is also shown in Figure 1(a). Figure 1(b) shows the binding energy curves for Pd, Au, and Pd-Au $L1_0$ structure calculated with Chen-Mobius inversion potentials and DFT method. From the figure, it can be seen that the developed potentials accurately reproduce DFT cohesive energy curves.

Table II. Related coefficient series of Chen-Mobius inverse formula for $L1_0$ super structure

n	1	2	3	4	5	6	7	8	9	10
$[b(n)]^2$	1	3	5	7	9	11	13	15	17	19
$r(n)$	8	16	16	32	24	16	48	32	32	48
$I(n)$	1/8	-1/4	-1/4	-1/2	1/8	-1/4	-3/4	1/2	-1/2	-3/4

3. MD simulations of Pd-Au NPs Melting

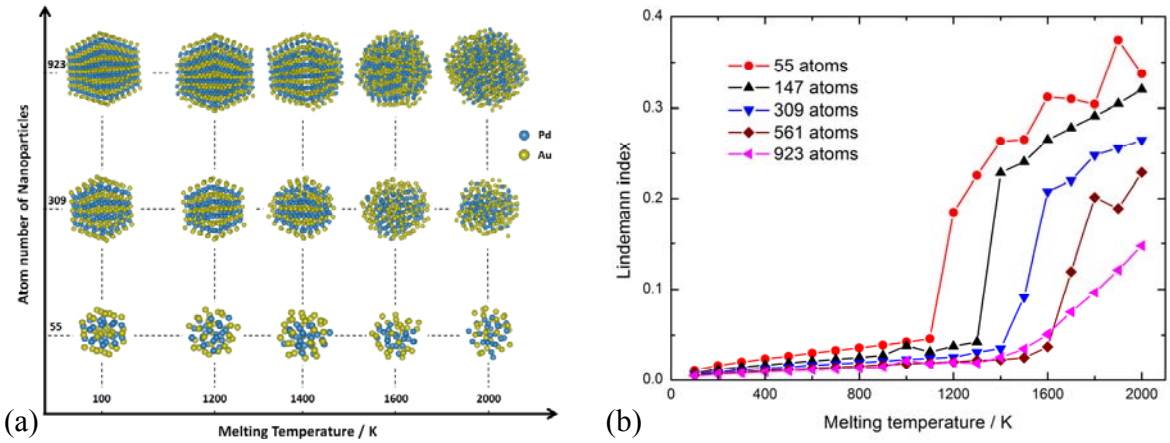

Figure 2. (Color online) (a) Morphology evolution of three selected sizes of Pd-Au NPs with increasing temperatures**.** (b) Variation of the *Lindemann index* as a function of temperature

Results of MD simulations for the melting of Pd-Au NPs are shown in Figure 2. Figure 2(a) shows snapshots of the morphology evolution with the increase of temperature for three selected sizes of Pd-Au NPs (55, 309 and 923 atoms), respectively. It can be seen that at low temperature, as 100K, the NPs keep their crystallographic $L1_0$ structures; with the temperature increasing, the NPs tend to become disordered gradually. When the temperature increases beyond a specified value, the NPs lose their crystallographic entirely and become molten state. It is clear that the larger NP has a higher threshold temperature. We could also observe that as temperature increases towards the melting point, the surface concentration of Au atoms increases. This is due to Au's lower surface energy as compared to Pd atoms and increased mobility at elevated temperature. As temperature increases even further, we observed increased Pd atoms on the surface, due to increased randomness at higher temperature.

To characterize the melting point more quantitatively, we calculated the *Lindemann index* of these five NPs. Figure 2(b) shows the variation as a function of temperature. Three distinct regions are revealed. At low temperatures the values of the *Lindemann index* are small, and rise up smoothly and slowly. When the temperature reaches a specified value, the *Lindemann index* has a sharp increase, as about 1200K for 55 atoms NP, 1300K for 147 atoms NP, and 1600K for 309 atoms NP, 1700K to 561 atoms NP. In the third stage, the *Lindemann index* continues to increase gradually but at a slope larger than that in the first stage. As first order approximation,

the melting point can be defined as the kink of the melting curve. It clearly shows that the melting points increase for larger size of NPs and get closer the value of bulk materials asymptotically. Such trend is consistent with previous reports, from both experiments[16] and computations[17]. As to 923-atoms NP, no exact kink which defines the melting point can be find in Fig 2(b). However, there is no essential difference with other NPs. It is predictable that the melting point should be larger than 1700K, which is agreeable with the figure. The possible reason for the missing of sharp increase is the larger surface energy caused by size increasing.

CONCLUSIONS

We have developed pair potentials for Pd-Pd, Au-Au and Pd-Au based on the Chen-Mobius lattice inversion formula and applied them to the study of Pd-Au NPs melting behavior. The Chen-Mobius inversion potentials accurately reproduces first-principles cohesive energy curves. Our MD simulation results explicitly show the particle size dependence of melting point via *Lindemann index* analysis and enrichment of Au atoms on the alloy NP surfaces.

ACKNOWLEDGMENTS

Bin Shan would like to acknowledge the support from Program for New Century Excellent Talents in University (NCET 01-24-110029). We thank Prof. Nanxian Chen, Prof. Jiang Shen, and Prof. Zhongyi Lu for fruitful discussions. Calculations presented in this paper were carried out using the High Performance Computing Center experimental testbed in SCTS/CGCL (see http://grid.hust.edu.cn/hpcc).

REFERENCES

1 N. Savastenko, H. R. Volpp, O. Gerlach, and W. Strehlau, Journal of Nanoparticle Research **10**, 277 (2008).
2 B. Shan, L. Wang, S. Yang, J. Hyun, N. Kapur, Y. Zhao, J. B. Nicholas, and K. Cho, Phys Rev B **80**, 35404 (2009).
3 M. S. Daw and S. M. Foiles and M. I. Baskes, Materials Science Reports **9**, 251 (1993).
4 S. Erko, Physics Reports **278**, 79 (1997).
5 N. Chen, Phys Rev Lett **64**, 3203 (1990).
6 C. Nan-xian and C. Zhao-dou and W. Yu-chuan, Phys Rev E **55**, R5 (1997).
7 J. Cai and X. Hu and N. Chen, J Phys Chem Solids **66**, 1256 (2005).
8 S. Zhang and N. Chen, Chem Phys **309**, 309 (2005).
9 S. Zhang and N. Chen, Phys Rev B **66**, 64106 (2002).
10 J. P. Perdew and K. Burke and M. Ernzerhof, Phys Rev Lett **77**, 3865 (1996).
11 W. Shinoda and R. DeVane and M. L. Klein, Soft Matter **4**, 2454 (2008).
12 M. L. Klein and W. Shinoda, Science **321**, 798 (2008).
13 S. Alavi and D. L. Thompson, The Journal of Physical Chemistry A **110**, 1518 (2006).
14 F. Ding and K. Bolton and A. Rosén, The European Physical Journal D - Atomic, Molecular, Optical and Plasma Physics **34**, 275 (2005).
15 F. A. Lindemann, Phys. Z. **11** (1910).
16 T. Bachels, U. G, H. Ntherodt, A. Sch, and R. Fer, Phys Rev Lett **85**, 1250 (2000).
17 F. G. Shi, J Mater Res **9**, 1307 (1994).